Measurement of two-qubit states by a two-island single-electron transistor

Tetsufumi Tanamoto
Corporate R&D Center, Toshiba Corporation, Saiwai-ku, Kawasaki 212-8582, Japan

Xuedong Hu
Department of Physics, University at Buffalo, SUNY, Buffalo, New York 14260-1500, USA
(Received 4 November 2003; published 2 March 2004)

We solve the master equations of two charged qubits measured by a single-electron transistor (SET) consisting of two islands. We show that in the sequential tunneling regime the SET current can be used for reading out results of quantum calculations and providing evidences of two-qubit entanglement, especially when the interaction between the two qubits is relatively weak compared to qubit-SET coupling.

DOI: 10.1103/PhysRevB.69.115301 PACS number(s): 73.21.La, 03.67.Mn, 81.07.Ta, 85.35.Gv

Quantum information processing in solid-state nanostructures has attracted widespread attention because of the potential scalability of such devices. Within this context, quantum measurement in mesoscopic systems is a crucial issue and is being carefully analyzed both experimentally[1–8] and theoretically,[9–18] so that proper measurements can be designed to extract the maximal amount of information contained in a solid-state qubit (or qubits). One prominent example is a single-electron transistor (SET), whose current is particularly sensitive to the charge degrees of freedom through gate potential variations on its central island(s).[19–21] Indeed, with a radio-frequency SET, electrons can be counted at frequencies up to 100 MHz,[4] so that if the states of a qubit can be distinguished by charge locations, a SET can be used to measure the qubit states.

Recently, two-qubit coherent evolution and possibly entanglement have been observed in capacitively coupled Cooper pair boxes.[22] The realization and detection of two-qubit entanglement are crucial milestones for the study of solid-state quantum computing. In this paper we study a scheme for the quantum measurement of two charge qubits ($N=2$), which can be extended to the detection of moderately larger number of qubits ($N>2$). Specifically, the target qubits being constantly measured are double dot charge qubits,[15] whose states are the different spatial distributions of the excess electron on the double dot. The quantum detector is a two-island SET ($N=2$), with each island coupled to a qubit capacitively, as illustrated in Fig. 1. Our objective is to demonstrate the capability of this two-island SET in detecting and differentiating two-qubit quantum states. In particular, we develop a master-equation formalism from microscopic Hamiltonian to describe the readout current of the SET in its sequential tunneling regime. Under the condition that the relaxation time of SET current is sufficiently long compared to the period of qubit oscillations, we clarify three major issues regarding the capability of the two-island SET layout: whether the two-qubit eigenstates $\{|00\rangle,|01\rangle,|10\rangle$, and $|11\rangle\}$ can be distinguished, whether entangled states and product states can be distinguished, and whether Zeno effect can be seen in the two qubits.[23]

The Hamiltonian for the combined two qubits and the two-island SET can be written as follows:

$$H=H_{\mathrm{qb}}+H_{\mathrm{set}}+H_{\mathrm{int}}, \tag{1}$$

where H_{qb}, H_{set}, and H_{int} are the Hamiltonians of the two qubits, the SET, and the interaction between the qubits and the SET, respectively. H_{qb} describes the two interacting (left and right, as illustrated in Fig. 1) qubits, each consisting of two tunnel-coupled quantum dots (QD's) and containing one excess charge:[15]

$$H_{\mathrm{qb}}=\sum_{\alpha=L,R}(\Omega_\alpha\sigma_{\alpha x}+\Delta_\alpha\sigma_{\alpha z})+J\sigma_{Lz}\sigma_{Rz}, \tag{2}$$

where Ω_L (Ω_R) and $\Delta_L(t)[\Delta_R(t)]$ are the inter-QD (but intraqubit) tunnel coupling and energy difference in the left (right) qubit. Here we use the spin notation such that $\sigma_{\alpha x}\equiv a_\alpha^\dagger b_\alpha+b_\alpha^\dagger a_\alpha$ and $\sigma_{\alpha z}\equiv a_\alpha^\dagger a_\alpha-b_\alpha^\dagger b_\alpha$ ($\alpha=L,R$), where a_α and b_α are the annihilation operators of an electron in the upper and lower QD's of each qubit. J is a coupling constant between the two qubits, originating from capacitive couplings in the QD system.[15] $|\uparrow\rangle$ and $|\downarrow\rangle$ refer to the two single-qubit states in which the excess charge is localized in the upper and lower dot, respectively. Δ_α ($\alpha=L,R$) are bias gate voltages applied on the qubits, which can be used to tune the qubit energy splittings and are used for the manipulation of these charge qubits during quantum calculations.[15] The SET part of the Hamiltonian H_{set} is written as

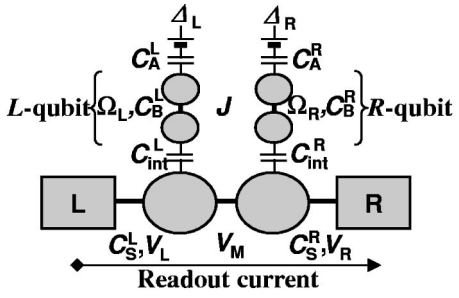

FIG. 1. Qubits are capacitively coupled to a two-island SET, which acts as a charge detector. $N(\geqslant 2)$ qubits are arranged between source and drain.

$$H_{\mathrm{set}}=\sum_{\alpha=L,R}\left[\sum_{i_\alpha,s}E_{i_\alpha}c^{\dagger}_{i_\alpha s}c_{i_\alpha s}+\sum_{s}E_{d_\alpha s}d^{\dagger}_{\alpha s}d_{\alpha s}+U_\alpha n_{\alpha\uparrow}n_{\alpha\downarrow}\right]$$
$$+\sum_{\alpha=L,R}\sum_{i_\alpha,s}V_{\alpha s}(c^{\dagger}_{i_\alpha s}d_{\alpha s}+d^{\dagger}_{\alpha s}c_{i_\alpha s})$$
$$+\sum_{s}V_{Ms}(d^{\dagger}_{Ls}d_{Rs}+d^{\dagger}_{Rs}d_{Ls}). \tag{3}$$

Here $c_{i_L s}$ ($c_{i_R s}$) is the annihilation operator of an electron in the i_Lth (i_Rth) level ($i_L(i_R)=1,\ldots,n$), in the left (right) electrode, d_{Ls} (d_{Rs}) is the electron annihilation operator of the left (right) SET island, $s\in\{\uparrow,\downarrow\}$ is the electron spin, and $n_{\alpha s}\equiv d^{\dagger}_{\alpha s}d_{\alpha s}$ is the number of electrons on each island. Here we assume only one energy level on each island. V_{Ls} (V_{Rs}) and V_{Ms} are the tunneling strength of electrons between left (right) electrode and the left (right) island and that between the two islands. $U_L(U_R)$ is the on-site Coulomb energy of double occupancy in the left (right) island. Finally, the interaction between the qubits and the SET, described by H_{int}, are capacitive couplings between the qubits and the two SET islands:

$$H_{\mathrm{int}}=\sum_{s}(E^{L}_{\mathrm{int}}d^{\dagger}_{Ls}d_{Ls}\sigma_{Lz}+E^{R}_{\mathrm{int}}d^{\dagger}_{Rs}d_{Rs}\sigma_{Rz}). \tag{4}$$

Consequently, the energy level of a SET island is raised by $E^{\alpha}_{\mathrm{int}}\sim eC^{\alpha}_{\mathrm{int}}C^{\alpha}_{\mathrm{A}}/C^{\alpha}_{\mathrm{S}}/(C^{\alpha}_{\mathrm{A}}C^{\alpha}_{\mathrm{int}}+C^{\alpha}_{\mathrm{B}}[C^{\alpha}_{\mathrm{A}}+C^{\alpha}_{\mathrm{int}}])$ if the charge in the corresponding qubit is located in the lower QD.[11] The electronic states of the qubits also influence the tunneling rates $\Gamma^{\alpha}(E)=2\pi\rho_{\alpha}(E)|V_{\alpha}(E)|^2$ (ρ_α are densities of states of the electrodes). If we define $\{|A\rangle\equiv|\downarrow\downarrow\rangle,\ |B\rangle\equiv|\downarrow\uparrow\rangle,\ |C\rangle\equiv|\uparrow\downarrow\rangle,\ |D\rangle\equiv|\uparrow\uparrow\rangle\}$, the tunneling rates would then satisfy the following relationships: $\Gamma^{L}_{A}=\Gamma^{L}_{B}<\Gamma^{L}_{C}=\Gamma^{L}_{D}$ and $\Gamma^{R}_{A}=\Gamma^{R}_{C}<\Gamma^{R}_{B}=\Gamma^{R}_{D}$.

Now we can construct the equations of the qubits-SET density-matrix elements governed by the above-mentioned Hamiltonian at $T=0$, following the procedure developed by Gurvitz.[9] The possible electronic states in the detector that we consider are shown in Fig. 2. Our derivation procedure is valid as long as the energy levels of the islands are inside the chemical potentials μ_L of the left electrode and μ_R of the right electrode, and the tunneling rates are much smaller than

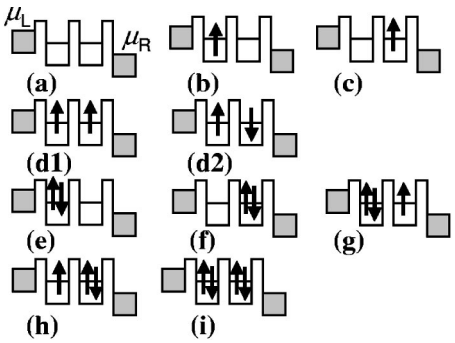

FIG. 2. Electronic states in the detector.

the chemical potential difference $\mu_L-\mu_R$, i.e., $\mu_L-\mu_R\gg\{\Gamma^{L},\Gamma^{R},V_M\}$.[24] We consider the following two transport processes separately. The first case is when the double-occupied states are energetically between μ_L and μ_R and all the electronic states in Fig. 2 take part in the tunneling (finite U model). The second case is when double occupancy of electrons [(e)–(i) in Fig. 2] is prohibited through sequential tunneling (infinite U model). Experimentally, these two cases are interchangeable by tuning the applied island gate voltages.[25]

The wave function $|\Psi(t)\rangle$ of the qubits-SET system can be expanded over the two-electron states of the qubits, the island states of the SET shown in Fig. 2, and all possible electrode states. More specifically, we choose $|0\rangle$ to refer to the initial ground state of the whole SET system where the two electrodes are filled with electrons up to μ_L and μ_R, respectively, and the two islands are empty of excess electrons. The basis states for the SET can then be constructed from $|0\rangle$ by moving electrons from the left electrode (with higher chemical potential) to the two islands and the right electrode. For convenience, we categorize the states by the number of electrons that have been transferred from the left to the right electrode:

$$|\Psi(t)\rangle=|\Psi_0(t)\rangle+|\Psi_1(t)\rangle, \tag{5}$$

where $|\Psi_0(t)\rangle$ is the part of the wave function where no electron reaches the right electrode and $|\Psi_1(t)\rangle$ represents the part of the wave function where more than one electron is transferred to the right electrode. $|\Psi_0(t)\rangle$ can be expressed as

$$|\Psi_0(t)\rangle=\sum_{z=A,B,C,D}\Bigg\{b^{(0)a,z}(t)+\sum_{ls}[b^{(0)b,z}_{ls}(t)d^{\dagger}_{Ls}c_{ls}+b^{(0)c,z}_{ls}(t)d^{\dagger}_{Rs}c_{ls}]+\sum_{l_1l_2s_1s_2}b^{(0)d,z}_{l_1l_2s_1s_2}(t)d^{\dagger}_{Ls_1}d^{\dagger}_{Rs_2}c_{l_1s_1}c_{l_2s_2}$$
$$+\sum_{l_1l_2}[b^{(0)e,z}_{l_1l_2}(t)d^{\dagger}_{L\uparrow}d^{\dagger}_{L\downarrow}c_{l_1\uparrow}c_{l_2\downarrow}+b^{(0)f,z}_{l_1l_2}(t)d^{\dagger}_{R\uparrow}d^{\dagger}_{R\downarrow}c_{l_1\uparrow}c_{l_2\downarrow}]+\sum_{l_1l_2l_3,s}[b^{(0)g,z}_{l_1l_2l_3s}(t)d^{\dagger}_{L\uparrow}d^{\dagger}_{L\downarrow}d^{\dagger}_{Rs}c_{l_1\uparrow}c_{l_2\downarrow}c^{\dagger}_{l_3s}$$
$$+b^{(0)h,z}_{l_1l_2l_3s}(t)d^{\dagger}_{R\uparrow}d^{\dagger}_{R\downarrow}d^{\dagger}_{Ls}c_{l_1\uparrow}c_{l_2\downarrow}c^{\dagger}_{l_3s}]+\sum_{l_1l_2l_3l_4}b^{(0)i,z}_{l_1l_2l_3l_4}(t)d^{\dagger}_{L\uparrow}d^{\dagger}_{L\downarrow}d^{\dagger}_{R\uparrow}d^{\dagger}_{R\downarrow}c_{l_1\uparrow}c_{l_2\downarrow}c_{l_3\uparrow}c_{l_4\downarrow}\Bigg\}|0\rangle|z\rangle, \tag{6}$$

where $b^{(0)a,z}(t)$, $b^{(0)b,z}_{ls}(t)$, ..., $b^{(0)i,z}_{l_1l_2l_3l_4}(t)$ are coefficients for the respective states. The superscripts refer to the number of electrons transferred, the SET island states (as illustrated in Fig. 2), and the four-qubit basis states. The subscripts refer to the left electrode states from which electrons tunnel into the islands. Thus each of the terms in $|\Psi_0(t)\rangle$ indicates a state with as

little as zero but up to four electrons jumping from the left electrode to the two SET islands. $|\Psi_1(t)\rangle$ can be expressed as

$$|\Psi_1(t)\rangle=\sum_{n=1}^{\infty}\sum_{\substack{z=A,\ldots,D\\ \beta_1\cdots\beta_n}}\Bigg\{b^{(n)a,z}_{\beta_1\cdots\beta_n}(t)+\sum_{ls}\,[b^{(n)b,z}_{ls\beta_1\ldots\beta_n}(t)d^{\dagger}_{Ls}c_{ls}+b^{(n)c,z}_{ls\beta_1\cdots\beta_n}(t)d^{\dagger}_{Rs}c_{ls}]$$

$$+\sum_{l_1l_2s_1s_2}b^{(n)d,z}_{l_1l_2s_1s_2\beta_1\cdots\beta_n}(t)d^{\dagger}_{Ls_1}d^{\dagger}_{Rs_2}c_{l_1s_1}c_{l_2s_2}+\sum_{l_1l_2}[b^{(n)e,z}_{l_1l_2\beta_1\cdots\beta_n}(t)d^{\dagger}_{L\uparrow}d^{\dagger}_{L\downarrow}c_{l_1\uparrow}c_{l_2\downarrow}+b^{(n)f,z}_{l_1l_2\beta_1\cdots\beta_n}$$

$$\times(t)d^{\dagger}_{R\uparrow}d^{\dagger}_{R\downarrow}c_{l_1\uparrow}c_{l_2\downarrow}]+\sum_{l_1l_2l_3s}[b^{(n)g,z}_{l_1l_2l_3s\beta_1\cdots\beta_n}(t)d^{\dagger}_{L\uparrow}d^{\dagger}_{L\downarrow}d^{\dagger}_{Rs}c_{l_1\uparrow}c_{l_2\downarrow}c^{\dagger}_{l_3s}+b^{(n)h,z}_{l_1l_2l_3s\beta_1\cdots\beta_n}(t)d^{\dagger}_{R\uparrow}d^{\dagger}_{R\downarrow}d^{\dagger}_{Ls}c_{l_1\uparrow}c_{l_2\downarrow}c^{\dagger}_{l_3s}]$$

$$+\sum_{l_1l_2l_3l_4}b^{(n)i,z}_{l_1l_2l_3l_4\beta_1\cdots\beta_n}(t)d^{\dagger}_{L\uparrow}d^{\dagger}_{L\downarrow}d^{\dagger}_{R\uparrow}d^{\dagger}_{R\downarrow}c_{l_1\uparrow}c_{l_2\downarrow}c_{l_3\uparrow}c_{l_4\downarrow}\Bigg\}\otimes\prod_{i=1}^{n}(c^{\dagger}_{l_i's_i'}c_{r_i's_i'})|0\rangle|z\rangle, \tag{7}$$

where $\beta_i\equiv(l_i',r_i',s_i')$ represent the electrode states involved in the electron transfers. Similar to the expression of the coefficients for $|\Psi_0(t)\rangle$, here $b^{(n)a,z}_{\beta_1\cdots\beta_n}(t),\ldots,$ $b^{(n)i,z}_{l_1l_2l_3l_4\beta_1\cdots\beta_n}(t)$ are coefficients for the states with n electrons transferred to the right electrode, and another 0–4 electrons jumped from the left electrode to the SET islands. The superscripts again refer to the number of transferred electrons, the SET island states, and the qubit basis states. The subscripts l_i and s_i refer to the left electrode states from which electrons tunnel into the islands, while the rest of the subscripts $\beta_1\cdots\beta_n$ indicate the electrode states of the electrons transferred from the left to the right electrode.

Substituting this wave function into the Schrödinger equation for the whole qubit-SET system, $i|\dot{\Psi}(t)\rangle=H|\Psi(t)\rangle$, we obtain a set of algebraic equations for the coefficients $b^{u,z}_{\beta}(t)$ [as we have mentioned above, β indicates the electrode states for the electrons, u is the quantum state of the SET islands (Fig. 2), and $z=A,B,C,D$ refers to the state of the qubits]. We assume that there is no magnetic field and electron tunneling is independent of spin. The density-matrix elements can then be defined as

$$\rho^{z_1z_2}_{u_1u_2}(t)\equiv\sum_{\beta}\int\frac{dEdE'}{4\pi^2}\tilde{b}^{u_1,z_1}_{\beta}(E)\tilde{b}^{u_2,z_2*}_{\beta}(E)e^{i(E-E')t}, \tag{8}$$

where $\tilde{b}^{u_1,z_1}_{\beta}(E)$ is a Laplace-transformed element of $b^{u_1,z_1}_{\beta}(t)$. After a lengthy calculation, we obtain 352 equations for density-matrix elements $\rho^{z_1z_2}_{u_1u_2}(t)$ (see the Appendix):

$$\dot{\rho}^{AA}_{aa}=-2\Gamma^L\rho^{AA}_{aa}-i\Omega_R(\rho^{BA}_{aa}-\rho^{AB}_{aa})-i\Omega_L(\rho^{CA}_{aa}-\rho^{AC}_{aa})$$
$$+\Gamma^R(\rho^{AA}_{cc\uparrow}+\rho^{AA}_{cc\downarrow}),$$

$$\dot{\rho}^{AB}_{aa}=[i(-J_A+J_B)-2\Gamma^L]\rho^{AB}_{aa}-i\Omega_R(\rho^{BB}_{aa}-\rho^{AA}_{aa})$$
$$-i\Omega_L(\rho^{CB}_{aa}-\rho^{AD}_{aa})+\Gamma^R(\rho^{AB}_{cc\uparrow}+\rho^{AB}_{cc\downarrow}),$$

$$\vdots$$

$$\dot{\rho}^{CD}_{ii}=2[i(-E^C_{d_L}-E^C_{d_R}+E^D_{d_L}+E^D_{d_R}-J_C+J_D)-\Gamma^{R'}]\rho^{CD}_{ii}$$
$$-i\Omega_R(\rho^{DD}_{ii}-\rho^{CC}_{ii})-i\Omega_L(\rho^{AD}_{ii}-\rho^{CB}_{ii})$$
$$+\Gamma^{L'}(\rho^{CD}_{hh\uparrow}+\rho^{CD}_{hh\downarrow}), \tag{9}$$

where $J_A=\Delta_L+\Delta_R+J$, $J_B=\Delta_L-\Delta_R-J$, $J_C=-\Delta_L+\Delta_R-J$, $J_D=-\Delta_L-\Delta_R+J$, $E^A_{d_L}=E^B_{d_L}=E_{d_L}+E^L_{\rm int}$, $E^C_{d_L}=E^D_{d_L}=E_{d_L}-E^L_{\rm int}$, $E^A_{d_R}=E^C_{d_R}=E_{d_R}+E^R_{\rm int}$, and $E^B_{d_R}=E^D_{d_R}=E_{d_R}-E^R_{\rm int}$. $\Gamma^{\alpha'}=0$ in infinite U model and $\Gamma^{\alpha'}=\Gamma^{\alpha}$ in finite U model. For simplicity we consider two identical qubits, with $E_{d_L}=E_{d_R}$ and $E_{\rm int}\equiv E^L_{\rm int}=E^R_{\rm int}$. The readout current $I(t)=e\dot{N}_R(t)$ is[9]

$$I(t)=\sum_{z=A,B,C,D}e\{\Gamma^R[\rho^{zz}_{cc\uparrow}+\rho^{zz}_{cc\downarrow}+\rho^{zz}_{d_{\uparrow\uparrow}d_{\uparrow\uparrow}}+\rho^{zz}_{d_{\downarrow\uparrow}d_{\downarrow\uparrow}}+\rho^{zz}_{d_{\uparrow\downarrow}d_{\uparrow\downarrow}}$$
$$+\rho^{zz}_{d_{\downarrow\downarrow}d_{\downarrow\downarrow}}+2\rho^{zz}_{ff}+\rho^{zz}_{gg\uparrow}+\rho^{zz}_{gg\downarrow}+2(\rho^{zz}_{hh\uparrow}+\rho^{zz}_{hh\downarrow})]$$
$$+2\Gamma^{R'}\rho^{zz}_{ii}\}. \tag{10}$$

We monitor the onset of the readout current to extract information of the qubit states. The initial state of the SET is such that there is no excess electron in the SET islands, which corresponds to state (a) in Fig. 2 and there is no current through the SET [see Eq. (10)]. The current begins to flow at $t=0$ and after a transient region saturates to a steady-state value. In the absence of the two-island SET, the qubits oscillate with frequencies $\sqrt{\Omega_\alpha^2+\Delta_\alpha^2}$. Their interaction with the dissipative current through the SET degrades the qubit coherent oscillations and drives the charge distribution towards uniformity in the qubits at $t\to\infty$. Conversely, in the absence of the qubits, the SET current saturates after $t\sim\Gamma^{-1}$, where $\Gamma\equiv\Gamma^L\Gamma^R/(\Gamma^L+\Gamma^R)$. The presence of the qubits and their charge oscillations modify the SET current through an effective gate potential on the islands. Figure 3 shows the time-dependent current characteristics of the infinite U model near $t\sim0$. To calculate the current when the qubit initial state is $|A\rangle$, for example, we set $b^{(0)a,A}(0)=1$ and the other coefficients zero in the total wave function

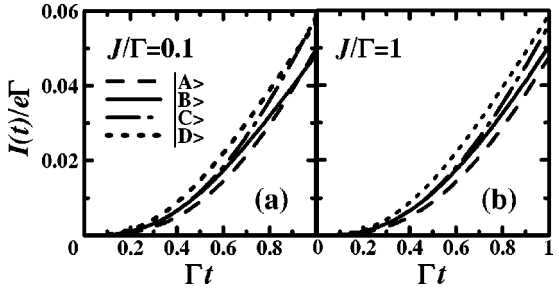

FIG. 3. Time-dependent readout current characteristics of the infinite U model for $|A\rangle=|\downarrow\downarrow\rangle$, $|B\rangle=|\downarrow\uparrow\rangle$, $|C\rangle=|\uparrow\downarrow\rangle$, $|D\rangle=|\uparrow\uparrow\rangle$ as initial states ($t=0$), where $\Omega_L=\Omega_R=0.75\Gamma$, $V_M=0.5\Gamma$, $E_{\rm int}^L=E_{\rm int}^R=0.2\Gamma$, $\Gamma_A^L=\Gamma_B^L=\Gamma_A^R=\Gamma_C^R=0.8\Gamma$, $\Gamma_C^L=\Gamma_D^L=\Gamma_B^R=\Gamma_D^R=1.2\Gamma$. (a) $J=0.1\Gamma$, (b) $J=\Gamma$.

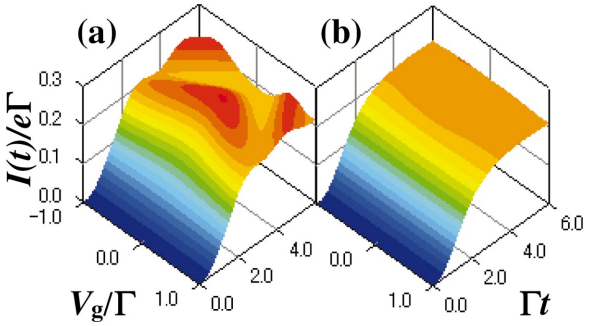

FIG. 4. (Color) Time-dependent readout current characteristics starting from (a) $|B\rangle$, (b) singlet state in the infinite U model for weak measurement case ($E_{\rm int}=0.2\Gamma<V_M=0.5\Gamma$) as a function of $V_{\rm g}=V_{\rm g}^L=V_{\rm g}^R$. Parameters are the same as those in Fig. 3.

[Eqs. (6) and (7)], which means that $\rho_{aa}^{AA}(0)=1$ and other density-matrix elements are zero at $t=0$. At small time t qubit state $|A\rangle$ suppresses the current the most while state $|D\rangle$ the least. The measurement time t_m that is required to resolve the states of qubits is estimated to be $t_{\rm m}^{-1}\sim\min\{E_{\rm int},\Gamma_A^L-\Gamma_D^L\}$ ($\sim 0.5^{-1}\Gamma$ in Fig. 3). The relative magnitude of the current changes with the coherent oscillations of qubits ($t>1/\Omega_\alpha$). Thus the SET current can be used to distinguish the four product states during $t_{\rm m}<t<1/\Omega_\alpha$. If the coherent oscillation of the qubits remains after $t>\Gamma^{-1}$, as in the present model,[26] we can discuss the quantum states of qubits using the steady current formula ($t\to\infty$) through the SET without the qubits:[9]

$$I_{\rm set}=\frac{e\Gamma V_M^2}{\epsilon_d^2\Gamma/(\Gamma^L+\Gamma^R)+V_M^2+\Gamma^L\Gamma^R/4}, \tag{11}$$

where $\epsilon_d\equiv E_{d_L}-E_{d_R}$ is the energy difference of the two islands. If $V_M\gg\Gamma,\epsilon_d,\Omega_\alpha$, the coupling between the two islands is strong and the current mainly reflects the bonding-antibonding state in the detector, which is not suitable for qubit measurements. We thus focus on the regime of $V_M<\Omega_\alpha,\Gamma$. Since $E_{d_L}^A-E_{d_R}^A=E_{d_L}^D-E_{d_R}^D=0$ and $E_{d_L}^B-E_{d_R}^B=E_{d_R}^C-E_{d_L}^C=2E_{\rm int}$, the different effects between $|A\rangle$ and $|D\rangle$ and that between $|B\rangle$ and $|C\rangle$ come from the differences in the tunneling rates. Moreover, the difference of $|A\rangle$ and $|D\rangle$ from $|B\rangle$ and $|C\rangle$ becomes obvious in the $E_{\rm int}>V_M$ region. Thus we call $E_{\rm int}>V_M$ strong measurement regime, where the four product states can be distinguished, in contrast to the weak measurement regime of $E_{\rm int}<V_M$.

We can distinguish the current of pure entangled states and that of pure product states by changing bias voltages $V_g^\alpha=\Delta_\alpha$ in the regime of $J/\Gamma\ll 1$, where the current depends on the change of qubit oscillation frequency ($\sim\sqrt{\Omega_\alpha^2+\Delta_\alpha^2}$). Figure 4(a) shows the current corresponding to the qubit $|B\rangle$ state in the weak measurement regime of the infinite U model. We also obtained similar results for the other product states $|A\rangle$, $|C\rangle$, and $|D\rangle$. In contrast, the readout current for a two-qubit entangled state is more uniform compared with the product states as entangled states generally have less distinct charge distributions. For example, the density-matrix elements for a singlet state $(|\uparrow\downarrow\rangle-|\downarrow\uparrow\rangle)/\sqrt{2}=(|C\rangle-|B\rangle)/\sqrt{2}$ of two free qubits ($H_{\rm int}=0$) satisfy $\dot\rho^{BB}+\dot\rho^{CC}-\dot\rho^{BC}-\dot\rho^{CB}=0$ ($\Delta_L=\Delta_R$), which suggests that entangled states such as the singlet state are less effective in influencing the readout current. We believe this ineffectiveness is related to the fact that logical states encoded in entangled states are less susceptible to environmental decoherence.[27] Indeed, the readout current of this entangled state is found to be uniform as shown in Fig. 4(b). We obtained similar results for the other Bell states, and there is no significant difference between the infinite U model and the finite U model in the weak measurement regime.

In the strong measurement regime ($E_{\rm int}>V_M$), the current is more sensitive to the charge distributions in the qubits, and there are differences between the infinite U model and finite U model. We can distinguish the four products more easily through the SET current, as shown in Figs. 5(a)–5(d). However, currents for the entangled states in the infinite U model show several similar peaks that reflect the qubit oscillations and cannot be easily distinguished from the product states. On the other hand, the finite U model shows distinct uniform structure compared with the current of the product states [Figs. 5(e) and 5(f)]. This shows that, in the finite U model, redistribution of the electrons through the two islands of the detector is energetically favorable under the rather uniform electric field generated by the entangled qubits. Figure 6(a) shows that the concurrence (a measure of entanglement[28] derived from reduced density matrix of two qubits after tracing over the detector components) of the two qubits disappears quickly in the cases of strong measurement. While the coherence quickly degrades, we can see the emergence of the Zeno effect, in which a continuous measurement slows down transitions between quantum states due to the collapse of the wave functions into observed states.[9,14] For instance, Fig. 6(b) shows that, as $E_{\rm int}$ increases, the oscillations of density-matrix elements of the qubits (e.g., ρ^{DD}) are delayed, which is a clear evidence of the slowdown described by the Zeno effect in the two qubits.

Our numerical results above are applicable to a wide range of pure product and entangled states. For example, in the entangled states $\cos\theta|\downarrow\uparrow\rangle+e^{i\varphi}\sin\theta|\uparrow\downarrow\rangle$, we found that the uniformity of the readout current holds approximately up to $|\theta\pm\pi/4|,|\varphi|<\pi/12$. The pure entangled states are more ro-

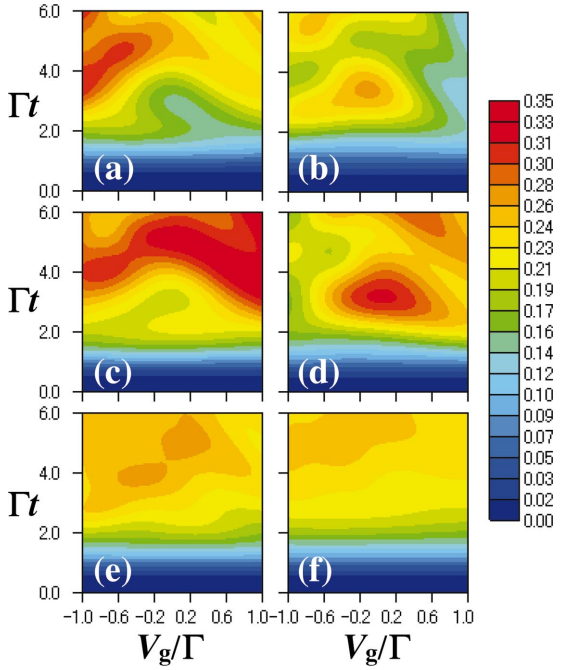

FIG. 5. (Color) Time-dependent readout current characteristics in the finite U model ($U=2\Gamma$) for strong measurement case ($E_{\rm int}=0.8\Gamma>V_M=0.5\Gamma$) as a function of $V_g=V_g^L=V_g^R$. The initial states are (a) $|A\rangle$, (b) $|B\rangle$, (c) $|C\rangle$, (d) $|D\rangle$, (e) triplet state, and (f) singlet state. Parameters other than $E_{\rm int}$ are the same as those in Fig. 3.

bust beyond the spatial distribution of the wave functions. Although the product states $\Pi_{\alpha=L,R}[\cos(\theta_\alpha/2)e^{-i\varphi_\alpha/2}|\uparrow\rangle_\alpha + \sin(\theta_\alpha/2)e^{i\varphi_\alpha/2}|\downarrow\rangle_\alpha]$ seem to have similarly uniform wave functions when $\theta_L=\pm\theta_R$ and $\varphi_L=\pm\varphi_R=0,\pi$ (compared to the entangled states mentioned above), the corresponding currents reflect the coherent oscillations of the qubits when the gate bias changes between $V_g^L=V_g^R$ and $V_g^L=-V_g^R$.

The initial state of each qubit is controlled by the gate biases Δ_L and Δ_R. The entangled states of the two qubits can be generated by tuning qubit gate biases and performing two-qubit operation (by controlling J) such as Controlled-NOT (C-NOT), as was theoretically demonstrated before.[15] In order to compare the experimental and theoretical results such as those presented in Figs. 3–5, it is necessary to measure the time-dependent currents at fixed gate biases Δ_α ($\alpha=L,R$),

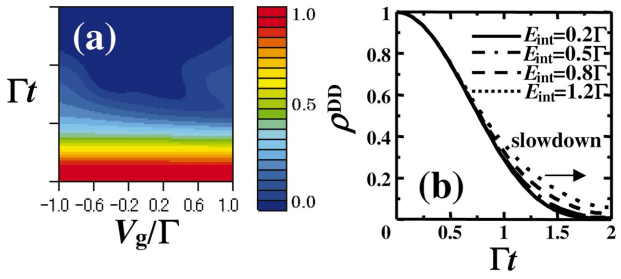

FIG. 6. (Color) (a) The concurrence of the singlet state. (b) Example of Zeno effect: oscillation of $\rho^{DD}(t)$ is delayed, where the initial state is $|D\rangle$ state [$\rho^{DD}(0)=1$]. Similar effects can be seen in other initial states. Parameters are the same as those in Fig. 5.

then repeat such measurements for a wide range of gate biases. Since the detection scheme discussed here is based on measuring small current differences in the transient regime, it is important to analyze whether the present-day technology can achieve the necessary sensitivity. The state of the art technology allows the measurement of 1 pA current with dynamics in the GHz frequency range with repeated measurement techniques.[1,2,8,29,30] According to our Figs. 3–5, our scheme requires measuring a 0.1 pA current that changes in the nanosecond time scale (assuming a Γ in the order of 100 MHz, a reasonable figure because $E_{\rm int}$ would be in the order of 100 MHz if all capacitances are 100 aF), which is at the edge of the current measurement technology. Thus, with a similar design of repeated measurement,[1,2,8,29,30] our detection scheme should be experimentally feasible in the near future.

In conclusion, we have solved master equations and described various time-dependent measurement processes of two charge qubits. The current through the two-island SET is shown to be an effective means to measure results of quantum calculations and entangled states.

We acknowledge discussions with N. Fukushima, S. Fujita, M. Ueda, T. Fujisawa, and S. Ishizaka, X.H. also acknowledges support from U.S. ARO and ARDA.

APPENDIX

The density-matrix elements we included in our dynamical study correspond to SET island states $(u_1,u_2)=\{(a,a), (b,b), (c,c), (b,c), (d_1,d_1), (d_2,d_2), (d_1,d_2), (e,e), (f,f), (e,d2), (f,d2), (e,f), (g,g), (h,h), (g,h), (i,i)\}$. Each element has a real and an imaginary part. The equations for these density-matrix elements are constructed following the method first adopted by Gurvitz (Ref. 9), from the time-dependent Schrödinger equations of the state coefficients [Eq. (8)]. The six off-diagonal elements mentioned above are included because they are connected to the diagonal elements by transferring one electron between the two islands or from one of the electrodes to one of the islands. In the equations for the density-matrix elements [Eq. (9)], a factor V_M corresponds to the case when an electron is transferred between the two islands, while a Γ_L or Γ_R factor indicates that an electron is transferred between an island and an electrode. The direction of tunneling from the electrodes is restricted to be from left to right in the equations for the density matrix. In other words, the bias between the left and right electrodes is set to be sufficiently large to suppress tunneling in the reversed direction.

The number of equations for the density matrix is arrived as follows. There are 16 diagonal elements for each island state in Fig. 2. For example, the diagonal matrix elements for state (a) include ρ_{aa}^{AA}, ρ_{aa}^{BB}, ρ_{aa}^{CC}, ρ_{aa}^{DD} (all real), ρ_{aa}^{AB}, ρ_{aa}^{AC}, ρ_{aa}^{AD}, ρ_{aa}^{BC}, ρ_{aa}^{BD}, and ρ_{aa}^{CD} (all complex). In addition, there are 32 elements corresponding to each off-diagonal island state pair. For example, the off-diagonal matrix elements for the (b)-(c) state has ρ_{bc}^{AA}, ρ_{bc}^{AB}, ρ_{bc}^{AC}, ρ_{bc}^{AD}, ρ_{bc}^{BB}, ρ_{bc}^{BC}, ρ_{bc}^{BD}, ρ_{bc}^{CC}, ρ_{bc}^{CD}, ρ_{bc}^{DD}, ρ_{cb}^{AB}, ρ_{cb}^{AC}, ρ_{cb}^{AD}, ρ_{cb}^{BC}, ρ_{cb}^{BD}, and ρ_{cb}^{CD} (all complex). Thus, in total we have $16\times10+32\times6=352$ equations.

[1] Y. Nakamura, Yu.A. Pashkin, T. Yamamoto, and J.S. Tsai, Phys. Rev. Lett. **88**, 047901 (2002).
[2] T. Fujisawa, D.G. Austing, Y. Tokura, Y. Hirayama and S. Tarucha, Nature (London) **419**, 278 (2002); Phys. Rev. Lett. **88**, 236802 (2002); T. Fujisawa, Y. Tokura, and Y. Hirayama, Phys. Rev. B **63**, 081304 (2001).
[3] W.G. van der Wiel, S. De Franceschi, J.M. Elzerman, T. Fujisawa, S. Tarucha, and L.P. Kouwenhoven, Rev. Mod. Phys. **75**, 1 (2003); S. Tarucha, D.G. Austing, T. Honda, R.J. van der Hage, and L.P. Kouwenhoven, Phys. Rev. Lett. **77**, 3613 (1996).
[4] A. Aassime, G. Johansson, G. Wendin, R.J. Schoelkopf, and P. Delsing, Phys. Rev. Lett. **86**, 3376 (2001); R.J. Schoelkopf, P. Wahlgren, A.A. Kozhevnikov, P. Delsing, and D.E. Prober, Science **280**, 1238 (1998).
[5] R. Aguado and L.P. Kouwenhoven, Phys. Rev. Lett. **84**, 1986 (2000).
[6] A.G. Huibers, M. Switkes, C.M. Marcus, K. Campman, and A.C. Gossard, Phys. Rev. Lett. **81**, 200 (1998).
[7] A. Yacoby, M. Heiblum, D. Mahalu, and H. Shtrikman, Phys. Rev. Lett. **74**, 4047 (1995).
[8] P.A. Cain, H. Ahmed, and D.A. Williams, J. Appl. Phys. **92**, 346 (2002).
[9] S.A. Gurvitz and Ya.S. Prager, Phys. Rev. B **53**, 15 932 (1996); B. Elattari and S.A. Gurvitz, Phys. Rev. Lett. **84**, 2047 (2000).
[10] H.S. Goan, G.J. Milburn, H.M. Wiseman, and H.B. Sun, Phys. Rev. B **63**, 125326 (2001); H.S. Goan and G.J. Milburn, *ibid.* **64**, 235307 (2001).
[11] Y. Makhlin, G. Schon, and A. Shnirman, Rev. Mod. Phys. **73**, 357 (2001).
[12] B.E. Kane, N.S. McAlpine, A.S. Dzurak, R.G. Clark, G.J. Milburn, He Bi Sun, and H. Wiseman, Phys. Rev. B **61**, 2961 (2000).
[13] D. Loss and E.V. Sukhorukov, Phys. Rev. Lett. **84**, 1035 (2000); H.A. Engel and D. Loss, Phys. Rev. B **65**, 195321 (2002).
[14] A.N. Korotkov, Phys. Rev. B **60**, 5737 (1999); Phys. Rev. A **65**, 052304 (2002).
[15] T. Tanamoto, Phys. Rev. A **64**, 062306 (2001); **61**, 022305 (2000).
[16] Y.X. Liu, S.K. Özdemir, M. Koashi, and N. Imoto, Phys. Rev. A **65**, 042326 (2002); L.F. Wei, S.Y. Liu, and X.L. Lei, *ibid.* **65**, 062316 (2002); A. Miranowicz, S.K. Özdemir, Y.X. Liu, M. Koashi, N. Imoto, and Y. Hirayama, *ibid.* **65**, 062321 (2002); X. Wang, M. Feng, and B.C. Sanders, *ibid.* **67**, 022302 (2003).
[17] E. Biolatti, R.C. Iotti, P. Zanardi, and F. Rossi, Phys. Rev. Lett. **85**, 5647 (2000); E. Biolatti, I. D'Amico, P. Zanardi, and F. Rossi, Phys. Rev. B **65**, 075306 (2002).
[18] B. Krummheuer, V.M. Axt, and T. Kuhn, Phys. Rev. B **65**, 195313 (2002); T. Itakura and Y. Tokura, *ibid.* **67**, 195320 (2003).
[19] M.H. Devoret and R.J. Schoelkopf, Nature (London) **406**, 1039 (2000).
[20] G. Johansson, A. Kack, and G. Wendin, Phys. Rev. Lett. **88**, 046802 (2002).
[21] A.B. Zorin, Phys. Rev. Lett. **76**, 4408 (1996); I. D'Amico and F. Rossi, Appl. Phys. Lett. **79**, 1676 (2001); **81**, 5213 (2002).
[22] Yu.A. Pashkin, T. Yamamoto, O. Astafiev, Y. Nakamura, D.V. Averin, and J.S. Tsai, Nature (London) **421**, 823 (2003); T. Yamamoto, Yu.A. Pashkin, O. Astafiev, Y. Nakamura, and J.S. Tsai, *ibid.* **425**, 941 (2003).
[23] L.M. Duan and G.C. Guo, Phys. Rev. A **57**, 2399 (1998).
[24] T.H. Stoof and Yu.V. Nazarov, Phys. Rev. B **53**, 1050 (1996).
[25] One limitation of the present formulation is that we cannot treat the boundary region where the energy of a double occupied island equals the Fermi energy of an electrode.
[26] We ignore other origins of decoherence, such as phonons, or trapped charges that generate the $1/f$ fluctuations.
[27] G.M. Palma, K.A. Suominen, and A.K. Ekert, Proc. R. Soc. London, Ser. A **452**, 567 (1996); P. Zanardi, Phys. Rev. A **57**, 3276 (1998); D.A. Lidar, I.L. Chuang, and K.B. Whaley, Phys. Rev. Lett. **81**, 2594 (1998).
[28] S. Hill and W.K. Wootters, Phys. Rev. Lett. **78**, 5022 (1997); W.K. Wootters, *ibid.* **80**, 2245 (1998).
[29] R.M. Potok, J.A. Folk, C.M. Marcus, V. Umansky, M. Hanson, and A.C. Gossard, Phys. Rev. Lett. **91**, 016802 (2003).
[30] S. Gardelis, C.G. Smith, J. Cooper, D.A. Ritchie, E.H. Linfield, Y. Jin, and M. Pepper, Phys. Rev. B **67**, 073302 (2003).